TE Modes of Graded-Index Slab Waveguides

D. MARCUSE

Abstract—An analysis of the TE modes of a slab waveguide with graded refractive-index distribution is presented. The refractive index is approximated by a piecewise-linear distribution for which exact solutions of the guided-wave problem can be obtained. For multimode guides, useful approximate solutions can be worked out with the help of the Wentzel–Kramers–Brillouin (WKB) approximation. A formula is given for the total number of guided TE modes supported by the waveguide.

The coupling efficiency of a prism coupler is investigated by studying the radiation losses of the guided modes escaping from the waveguide through the coupling prism. It is found that the radiation losses of the modes of the graded-index waveguide are more nearly constant than those of the asymmetric slab waveguide.

Introduction

WAVEGUIDES for integrated-optics applications can be made in many different ways. The most widely used methods of waveguide fabrication utilize the deposition of a dielectric material on a dielectric substrate of lower refractive index [1]–[3]. The resulting two-dimensional guidance structure consists of a refractive-index distribution that is constant in three different regions and jumps discontinuously at the interfaces between the guiding layer and the two regions bordering on it from above and below. Wave guidance in these asymmetric slab waveguides is well understood [4].

A different approach to the fabrication of integrated-optics waveguides consists of diffusing a suitable material into a substrate with the objective of increasing the refractive index near its surface. Kaminow and Carruthers [5] used the opposite approach and increased the refractive index of $LiNbO_3$ and $LiTaO_3$ crystals by out-diffusion of Li_2O from the surface [5]. Either method results in a slab waveguide with a graded-index profile.

In this paper we give a description of the guided modes of a graded-index slab waveguide that is based on approximating the actual refractive-index distribution by four straight line segments. The resulting boundary value problem can be solved exactly in terms of Bessel functions or to a very satisfactory approximation by means of the Wentzel–Kramers–Brillouin (WKB) method. Both methods of solution are described.

An important question concerns the efficiency with which the modes of graded-index waveguides can be excited by means of a prism coupler. In order to characterize the coupling efficiency of a prism coupler we calculate the attenuation coefficient of a guided wave losing power by radiation as it travels underneath the coupling prism located at the surface of the waveguide. This radiation loss coefficient is a measure of the coupling strength. If the wave cannot radiate out of the waveguide through the coupling prism it cannot be excited by shining light into the prism. On the other hand, if all the power of a guided wave leaks out of the waveguide in a distance short compared to the length of the coupling prism it is possible to excite this wave with a very high efficiency by shining light into the prism.

Manuscript received April 9, 1973.

The author is with Bell Laboratories, Crawford Hill Laboratory, Holmdel, N. J. 07733.

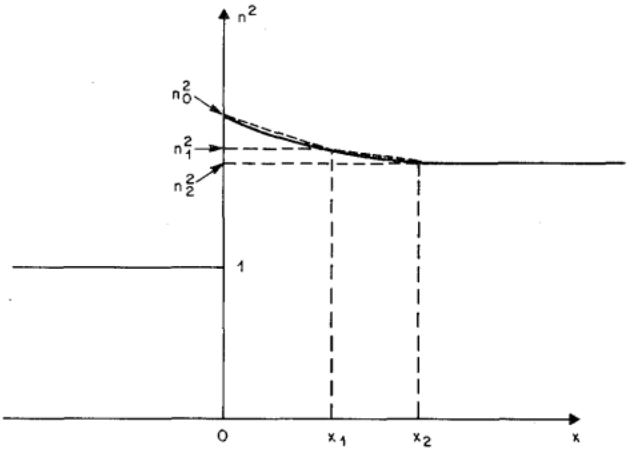

Fig. 1. Profile of the square of the refractive index of the graded-index slab waveguide. The dotted line represents the piecewise-linear approximation.

We find an interesting dependence of the radiation-loss coefficient on mode number. Whereas the attenuation coefficient increases with increasing mode number for the usual asymmetric slab waveguide, this coupling coefficient is much more nearly independent of mode number for the modes of the graded-index slab waveguide. This property of the graded-index modes is advantageous since it means that all the modes of this guide can be excited with nearly equal efficiency simply by adjusting the coupling angle of the incident laser beam.

The solution of the boundary-value problem is limited to TE modes. TM modes can, of course, be treated similarly. The total number of guided TE modes that the waveguide can support is expressed by a simple formula.

Piecewise-Linear Refractive-Index Approximation

The square of the refractive-index distribution of the graded-index slab waveguide is shown in Fig. 1. The surface $x = 0$ coincides with the top surface of the waveguide. In the region $x < 0$ we have air and in the region $x > 0$ the square of the refractive index decreases from its maximum value n_0^2 at $x = 0$ to the value n_2^2 at $x = \infty$. The dotted line indicates the approximation to the square of the actual index distribution by two piecewise-linear line segments. Analytically, we have the following approximate descrip-

tion of the square of the refractive-index distribution

$$n^2(x) = \begin{cases} 1, & -\infty < x < 0 \\ n_0^2 + (n_1^2 - n_0^2)\dfrac{x}{x_1}, & 0 < x < x_1 \\ n_1^2 + (n_2^2 - n_1^2)\dfrac{x - x_1}{x_2 - x_1}, & x_1 < x < x_2 \\ n_2^2, & x_2 < x < \infty. \end{cases} \quad (1)$$

For most practical purposes it is safe to assume that n_0 and n_1 differ only very slightly from n_2 so that we can use the approximation

$$n(x) = \begin{cases} 1, & -\infty < x < 0 \\ n_0 + (n_1 - n_0)\dfrac{x}{x_1}, & 0 < x < x_1 \\ n_1 + (n_2 - n_1)\dfrac{x - x_1}{x_2 - x_1}, & x_1 < x < x_2 \\ n_2, & x_2 < x < \infty. \end{cases} \quad (2)$$

The guided-wave problem requires only knowledge of the square of the refractive-index distribution. However, (2) is convenient to obtain the necessary parameters from refractive-index measurements.

Exact Description of TE Modes

The TE modes of the graded-index slab waveguide are obtained as solutions of the following equations [6]

$$\frac{d^2E_y}{dx^2} + (n^2(x)k^2 - \beta^2)E_y = 0 \quad (3)$$

$$H_x = -\frac{i}{\omega\mu_0}\frac{\partial E_y}{\partial z} \quad (4)$$

$$H_z = \frac{i}{\omega\mu_0}\frac{\partial E_y}{\partial x} \quad (5)$$

with

$$k^2 = \omega^2\epsilon_0\mu_0 = \left(\frac{2\pi}{\lambda_0}\right)^2. \quad (6)$$

The z and time dependence of the wave is assumed to be given by the factor

$$\exp[i(\omega t - \beta z)] \quad (7)$$

which is omitted from the equations for brevity.

The TE mode has only the three nonvanishing field components indicated in (3)–(5). The wave propagates in the z direction and there is no field variation in the y direction.

The reduced-wave equation (3) can be solved for a piecewise-linear distribution of n^2. The solution can be expressed in terms of Bessel functions

$$E_y = A_1 \exp(\gamma x), \quad \text{for} \quad -\infty < x < 0 \quad (8)$$

$$E_y = A_2\sqrt{u}\, J_{1/3}\left(\frac{2}{3|\eta|}u^{3/2}\right) + A_3\sqrt{u}\, J_{-1/3}\left(\frac{2}{3|\eta|}u^{3/2}\right), \quad 0 < x < x_1 \quad (9)$$

$$E_y = A_4\sqrt{v}\, J_{1/3}\left(\frac{2}{3|\Delta|}v^{3/2}\right) + A_5\sqrt{v}\, J_{-1/3}\left(\frac{2}{3|\Delta|}v^{3/2}\right), \quad x_1 < x < x_2 \quad (10)$$

$$E_y = A_6 \exp[-\theta(x - x_2)], \quad x_2 < x < \infty \quad (11)$$

with the abbreviations

$$\gamma^2 = \beta^2 - k^2 \quad (12)$$

$$\theta^2 = \beta^2 - n_2^2k^2 \quad (13)$$

$$\eta = \frac{n_1^2 - n_0^2}{x_1}k^2 \quad (14)$$

$$\Delta = \frac{n_2^2 - n_1^2}{x_2 - x_1}k^2 \quad (15)$$

$$u = n_0^2k^2 - \beta^2 + \eta x \quad (16)$$

and

$$v = n_1^2k^2 - \beta^2 + (x - x_1)\Delta. \quad (17)$$

The fact that we have used $n = 1$ for the index of the region $x < 0$ is no restriction on the generality of our problem. We need only consider k to be the propagation constant n_3k of plane waves in the medium at $x < 0$ (instead of the vacuum plane-wave propagation constant) to include an arbitrary but constant value n_3 of the refractive index and in addition replace n_i with n_i/n_3.

The amplitude coefficients and the propagation constant β are determined in the usual way by requiring continuity of the tangential components E_y and H_z at the interfaces $x = 0$, $x = x_1$, and $x = x_2$. We thus obtain six homogeneous equations for the six amplitude coefficients A_i. The solution of the homogeneous-equation system

$$\sum_j c_{ij}A_j = 0 \quad (18)$$

is given in the Appendix. The eigenvalue equation for the determination of β follows from the requirement that the system determinant must vanish

$$\det(c_{ij}) = 0. \quad (19)$$

The expressions for the exact solution of the graded-index

slab waveguide with piecewise-linear index distribution are cumbersome. However, computer solutions of the eigenvalue equation (19) can be obtained. But in addition to being awkward in appearance the exact solutions suffer from another difficulty. The sign of either $u(x)$ or $v(x)$ of (16) and (17) changes somewhere in the range of x values. The point $x = x_t$ at which either $u(x)$ an $v(x)$ vanish corresponds to the point at which a corresponding ray of a ray-optics solution of the graded-index problem would turn around in its trajectory that takes it from the surface $x = 0$ back toward this surface. As $u(x)$ or $v(x)$ change signs the arguments of the Bessel functions change from real to imaginary values. This change causes the Bessel function to change from an oscillatory to an exponentially growing function. Actually, both $J_{1/3}$ and $J_{-1/3}$ are composed of exponentially growing and decreasing functions for large imaginary values of their argument. The superposition of these functions as it appears in (9) or (10) tends to decrease rapidly as we move away from the turning point where the argument changes from real to imaginary values. The exponentially growing parts of the Bessel functions of imaginary arguments must thus cancel each other. When the exact equations are programmed into a computer this feature of the solution gives rise to very large roundoff errors. The growing terms grow to large values so that their differences that must nearly cancel eath other become very inaccurate. This problem prevents us from evaluating the exact solution for large numbers of guided modes. The exact solution can be evaluated easily only for guides supporting one or two modes. For many modes we must look to a different approach. The WKB approximation that was originally developed for problems in quantum mechanics is ideally suited for our purposes [7]. This approximation improves as the number of guided modes increases. The WKB approximation thus complements the exact solution.

WKB Approximation

The WKB approximation works well if the change of the refractive index is slow compared to the wavelength. For most graded-index slab waveguides that support many guided modes, this requirement is well satisfied. Only at the surface of the slab at $x = 0$ do we encounter a large, discontinuous change of the refractive index. We handle this problem in the usual way by matching the solution for $x < 0$ to the solution obtained from the WKB method for $x > 0$ by means of boundary conditions. We thus use an exact solution of the wave equation in the region $x < 0$ and the WKB approximation for $x > 0$.

$$E_y = A \exp(\gamma x), \qquad x < 0 \tag{20}$$

$$E_y = B\left(\frac{\kappa_0}{\kappa(x)}\right)^{1/2} A \cos\left(\frac{\pi}{4} - \phi(x)\right), \qquad 0 < x < x_t \tag{21}$$

$$E_y = \frac{B}{2i}\left(\frac{\kappa_0}{|\kappa(x)|}\right)^{1/2} A \exp\left\{-\int_{x_t}^{x} |\kappa(x)|\, dx\right\}, \qquad x_t < x < \infty. \tag{22}$$

The quantity B is defined by (28). The definition of γ is given by (12) and the additional definitions are

$$\kappa_0^2 = n_0^2 k^2 - \beta^2 \tag{23}$$

$$\kappa(x) = \sqrt{n^2(x)k^2 - \beta^2} \tag{24}$$

$$\phi(x) = \int_x^{x_t} \kappa(x)\, dx. \tag{25}$$

The turning point x_t is defined by the equation

$$\kappa(x_t) = 0. \tag{26}$$

The requirement that E_y and H_z remain continuous at $x = 0$ leads to the eigenvalue equation

$$\tan\left(\phi(0) - \frac{\pi}{4}\right) = \frac{\gamma}{\kappa_0} + \frac{\eta}{4\kappa_0^3}. \tag{27}$$

An alternate form of the eigenvalue equation can be obtained by solving (27) for the cosine function:

$$\frac{1}{B} = \cos\left(\phi(0) - \frac{\pi}{4}\right) = \frac{1}{\sqrt{1 + \left(\frac{\gamma}{\kappa_0} + \frac{\eta}{4\kappa_0^3}\right)^2}}. \tag{28}$$

Equations (21) and (22) fail at $x = x_t$ since the amplitude of the electric-field component is seen to have a pole at this point. However, if the refractive index distribution is replaced by a linear approximation in the vicinity of $x = x_t$ the WKB approximation holds everywhere and in the vicinity of $x = x_t$ we have

$$E_y = \frac{1}{2i}\sqrt{\frac{\pi}{3}}\,\sqrt{\kappa_0}\, B\sqrt{x_t - x}\, A \cdot \{\exp[i(2\pi/3)] H_{1/3}^{(1)}[\tfrac{2}{3} g(x_t - x)^{3/2}] + \exp[i(\pi/3)] H_{1/3}^{(2)}[\tfrac{2}{3} g(x_t - x)^{3/2}]\} \tag{29}$$

where $H_{1/3}^{(1)}$ and $H_{1/3}^{(2)}$ are the Hankel functions of $\frac{1}{3}$ order and of the first and second kind. The constant g is defined as

$$g = \left\{\left[2n(x)\left|\frac{dn}{dx}\right|\right]_{x=x_t}\right\}^{1/2} k. \tag{30}$$

The value of E_y at $x = x_t$ can thus be obtained from (29)

$$E_y = \sqrt{\kappa_0}\, B A \frac{\Gamma\left(\frac{1}{3}\right)\sin\frac{\pi}{6}}{\sqrt{3\pi}\, g^{1/3}} \tag{31}$$

where $\Gamma(x)$ is the γ-function.

The formulation of the WKB approximation presented so far is quite general and applies to any refractive-index distribution in the region $x > 0$. For arbitrary $n(x)$ the integrals in (22) and (25) usually cannot be solved in closed form so that the piecewise-linear refractive-index approximation is useful even in this case. The point $x = x_t$ is

different for each mode so that we must consider the cases $x_0 < x_t < x_1$ and $x_1 < x_t < x_2$. We thus obtain for the important phase parameter

$$\phi(0) = \begin{cases} -\frac{2}{3\eta}\kappa_0^3, & 0 < x_t < x_1 \\ -\frac{2}{3\eta}\left\{\kappa_0^3 + \frac{\eta - \Delta}{\Delta}(\kappa_0^2 + \eta x_1)^{3/2}\right\}, & x_1 < x_t < x_2. \end{cases} \quad (32)$$

The parameters η and Δ are defined by (14) and (15). They are both inherently negative quantities. The propagation constant β is determined by substitution of (32) into (27). The resulting eigenvalue equation can be solved with the help of a computer.

For guided modes that are far from cutoff we have $\gamma/\kappa_0 \gg 1$ so that an approximate solution of (27) is

$$\phi(0) = \left(2\nu + \frac{3}{2}\right)\frac{\pi}{2} \quad (33)$$

with $\nu = 0, 1, 2, \cdots$. This approximation can be used to determine the total number of guided modes that the waveguide can support. The lowest order guided mode has the largest propagation constant while the propagation constant of the highest order mode must be close to

$$\beta_N = n_2 k. \quad (34)$$

We thus obtain from (32)–(34), with $\nu + 1 = N$, the following formula for the total number of guided TE modes

$$N = -\frac{2k^3}{3\pi\eta}\left[(n_0^2 - n_2^2)^{3/2} + \frac{\eta - \Delta}{\Delta}(n_1^2 - n_2^2)^{3/2}\right] + \frac{1}{4}. \quad (35)$$

The total number of modes is the nearest integer that is smaller than the right-hand side of (35). The normalization of the modes (20)–(22) is achieved by evaluating the integral

$$P = -\frac{1}{2}\,\mathrm{Re}\left\{\int_{-\infty}^{\infty} E_y H_z^*\, dx\right\} = \frac{\beta}{2\omega\mu_0}\int_{-\infty}^{\infty} |E_y|^2\, dx. \quad (36)$$

Since the integral leads to the incomplete γ-function it is easiest to perform the integration numerically.

A comparison of the exact theory and the WKB approximation is shown in Fig. 2. To normalize the fields we used

$$\sqrt{P\omega\mu_0} = 1\ \mathrm{V/m}. \quad (37)$$

The parameter P indicates not the total power but the power per unit length (in the y direction). The solid line in Fig. 2 indicates the WKB approximation. The curve

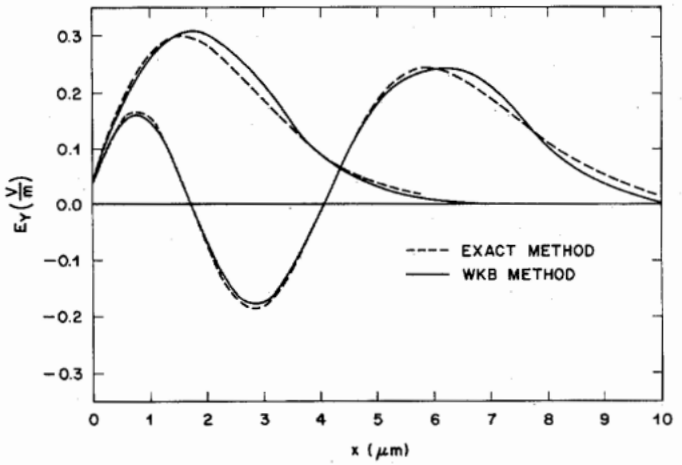

Fig. 2. Comparison of the WKB approximation (solid line) and the exact solution (dotted line) for mode 1 and mode 3 of a three-mode graded-index guide.

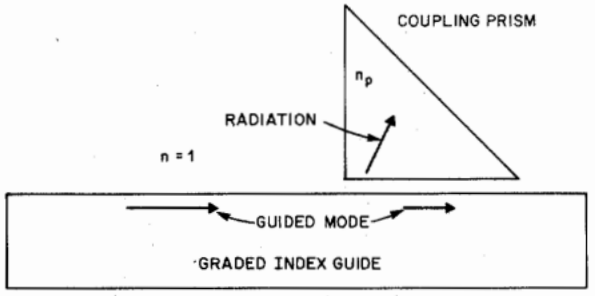

Fig. 3. Geometry of the coupling prism and the graded-index waveguide.

was drawn by using the value (31) at $x = x_t$ to continue the function E_y graphically through the point where (20)–(22) fail to apply. The normalization was based on numerical integration of (36) with a resulting inaccuracy at the point $x = x_t$. The slight error that results from this normalization procedure becomes apparent by a comparison of the maxima and the minima of the solid and the dotted curves. The latter was obtained from the exact solution (8)–(11). Fig. 2 shows the first and third guided TE modes of a three-mode graded-index guide. The agreement between the WKB approximation and the exact solution is quite good. The discrepancy between the two curves, that is apparent on the extreme right-hand side of the figure, is caused by the roundoff problem of the numerical evaluation of the exact theory that was discussed earlier.

Radiation Loss

In order to obtain an indication of the efficiency with which the modes of the graded-index slab waveguide can be excited we calculate the loss caused by the presence of the coupling prism on top of the waveguide as shown in Fig. 3.

It is assumed that a guided mode approaches the prism from the left. Before the field reaches the prism all its power is confined to the waveguide by total internal reflection at the top surface of the guide. As the wave travels under the prism some of its power leaks out into the prism since the evanescent-field tail (8) or (20) in the

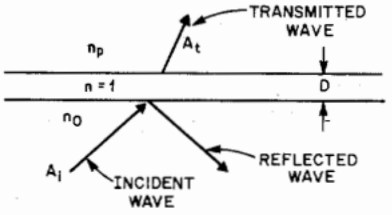

Fig. 4. This figure shows a plane wave that is reflected and transmitted at an air gap between two dielectric media.

air gap between prism and waveguide excites a radiation field in the prism. The amount of power outflow into the prism determines the radiation-loss coefficient.

We determine the power that is lost per unit length by considering the reflection and transmission of a plane wave at the interface shown in Fig. 4. A straightforward plane-wave analysis leads to the relation

$$A_t = \frac{-2i\kappa_0\gamma}{(\kappa_0\sigma - \gamma^2)\sinh\gamma D - i\gamma(\sigma + \kappa_0)\cosh\gamma D} A_i \quad (38)$$

where A_i and A_t are the amplitudes of the incident and transmitted plane waves. The parameters γ and κ_0 are defined by (12) and (23) and σ is the transverse propagation parameter in the prism with refractive index n_p,

$$\sigma^2 = n_p^2 k^2 - \beta^2. \quad (39)$$

The power attenuation coefficient α is obtained as the ratio of power outflow per unit length (in the z direction) divided by the power carried in the guide

$$\alpha = \frac{\sigma |A_t|^2}{2\omega\mu_0 P}. \quad (40)$$

According to the WKB approximation (21) the amplitude A_i of the incident wave is related to the amplitude A of the wave in the air gap by the relation

$$A_i = \tfrac{1}{2} B A. \quad (41)$$

The radiation-loss amplitude coefficient thus follows from (38)–(41)

$$\alpha = \frac{B^2\sigma\gamma^2\kappa_0^2 |A|^2}{2\omega\mu_0 P\{[(\kappa_0\sigma - \gamma^2)\sinh\gamma D]^2 + [\gamma(\sigma + \kappa_0)\cosh\gamma D]^2\}}. \quad (42)$$

The derivation of this expression was based on the assumption that a plane wave impinges on the air gap between waveguide and prism. The wave in the graded-index guide is not composed of plane waves. However, for high-order guided modes the wave near the top surface of the waveguide more nearly approaches a plane wave. Our approximate expression is thus more accurate for high-order modes. However, we are using (42) to estimate the radiation power loss for all the modes.

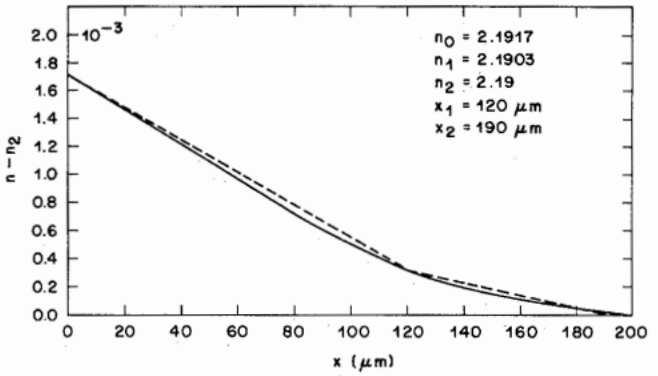

Fig. 5. Index distribution measured by Kaminow and Carruthers [5] (solid line). The dotted line is a piecewise-linear approximation. $n_0 = 2.1917$, $n_1 = 2.1903$, $n_2 = 2.19$, $x_1 = 120\ \mu m$, $x_2 = 190\ \mu m$.

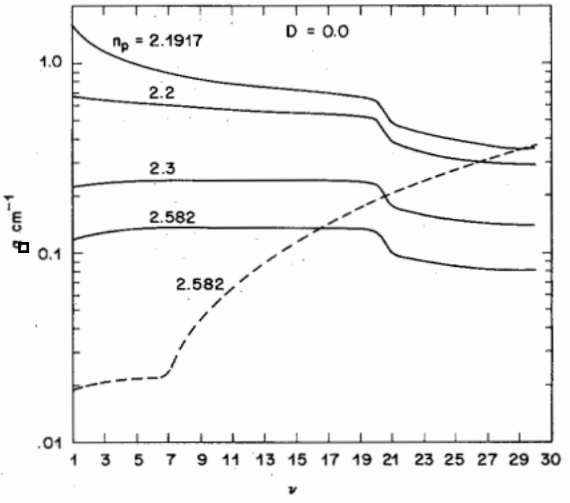

Fig. 6. Radiation-loss coefficient α as a function of mode number ν for several values of the refractive index of the prism for zero air gap, $D = 0$. The dotted line represents the result for an (almost) asymmetric slab waveguide.

Numerical Results

The solid curve in Fig. 5 is a plot of the refractive-index distribution of the graded-index slab waveguide produced by Kaminow and Carruthers [5] by outdiffusion of Li_2O from $LiTaO_3$. The dotted line is the piecewise-linear approximation of the refractive-index distribution.

It follows from (35) that 30 modes can propagate in this waveguide at a free-space wavelength of $\lambda_0 = 0.6328\ \mu m$ corresponding to $k = 9.9292\ \mu m^{-1}$.

Fig. 6 shows the radiation-loss coefficient as a function of mode number for several values of the refractive index of the prism for vanishing air gap. The loss is plotted in units of cm^{-1}, the power loss, in decibels per centimeter, follows from the figure by multiplication with 4.34. The figure shows several interesting features. The radiation loss increases with decreasing refractive index of the prism. However, even if the refractive index of the prism matches the refractive index of the top layer of the waveguide the radiation loss is still only moderately high. For the lowest index value of $n_p = 2.1917$ the loss

decreases with mode number. For the lowest order mode a distance of 0.67 cm is required until the power decreases to $1/e$ of its initial value. For the highest order mode this distance has increased to 2.8 cm. The highest refractive index shown in the figure, $n_p = 2.582$, corresponds to a rutile prism. The radiation loss is almost independent of mode number for the first 19 modes. The sudden drop of the loss curve between mode 19 and 20 is caused by the fact that the turning point has moved from the first straight line segment in Fig. 5 to the second straight line segment with a more gentle slope. The reduced slope of the refractive-index distribution causes the field to reach deeper into the waveguide so that the ratio of the power density carried in the top layer of the guide to the total power is reduced. This smaller ratio causes the power loss from the waveguide to be smaller. The shape of the loss curve would of course be different for the actual index distribution. The sudden drop would be replaced by a certain average slope of the curve. However, it is apparent that the loss is not very strongly dependent on mode number.

The dotted line in Fig. 6 shows the radiation loss from a slab waveguide with an almost rectangular index profile approximating the asymmetric slab waveguide. This curve was also obtained with the help of the WKB approximation by letting the first line segment of the piecewise-linear refractive-index distribution be almost horizontal and allowing the second part to drop off abruptly. The dotted curve shows that the radiation losses increase sharply with increasing mode number for the asymmetric slab waveguide. The step in the curve occurs when the turning point x_t moves from the almost horizontal line section to the almost vertical line section of the refractive-index distribution. From the point of view of mode excitation with a prism coupler the graded-index guide is more favorable since it allows a more nearly constant excitation efficiency for all the modes. This dependence of the radiation loss on mode number can be explained as follows. Higher order modes impinge on the interface at steeper angles, but the resulting increase in power outflow is partially compensated by the fact that the higher order modes extend deeper into the guide carrying relatively more power.

Fig. 7 shows the radiation loss versus mode number for several values of the gap width D for a prism whose index, $n_p = 2.1917$, matches the index of the top layer of the waveguide. The dependence of radiation loss on gap width is very pronounced. The very moderate gap width $D = 0.05$ μm (this is only 0.08 of the wavelength) causes a decrease of the radiation-loss coefficient by two orders of magnitude. The coupling efficiency is impractically low in this case since it is impossible to feed appreciable amounts of power into a waveguide when the inverse process of power loss from the guide requires 5 m for a decrease of the power to $1/e$ of its initial value.

Fig. 8 shows the dependence of radiation loss on gap width as a parameter for a larger refractive index of the prism, $n_p = 2.582$, than in Fig. 7. The dependence of the loss on the gap width is less pronounced in this case.

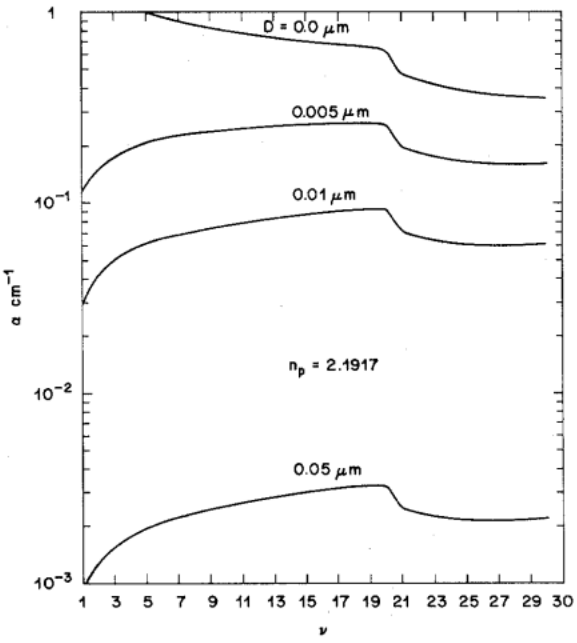

Fig. 7. Radiation loss α as a function of mode number ν for several values of the gap width D for $n_p = 2.1917$.

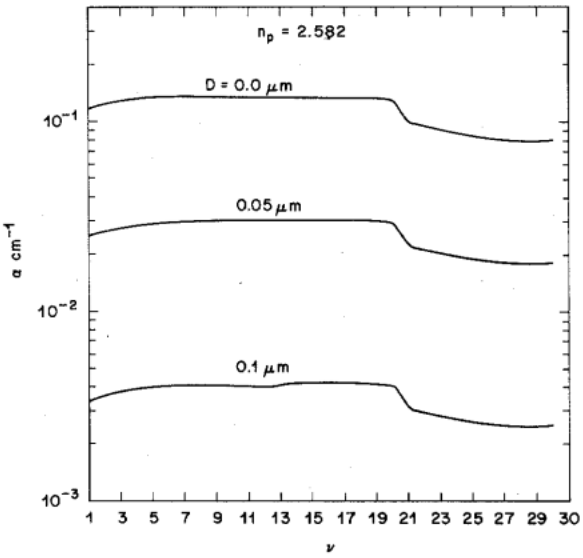

Fig. 8. Same as Fig. 7 for $n_p = 2.582$.

Conclusions

Effective waveguides for integrated-optics applications can be made with a graded refractive-index distribution. A piecewise-linear approximation of the actual index distribution permits an exact solution. This solution is useful for determining the performance of a single mode guide. For multimode operation solutions obtained with the WKB approximation are more useful. A closed-form expression for the total number of modes that can be supported by the waveguide is obtained.

The graded-index slab waveguide has the advantage over a multimode asymmetric slab waveguide with discontinuous but piecewise constant refractive-index profile that

all its modes can be excited with more nearly equal efficiency by a prism coupler. The radiation losses for the guided modes escaping through the coupling prism are plotted as functions of mode number for several values of the refractive index of the prism and for several values of the gap width.

Appendix

With the abbreviations

$$a = \frac{2}{3\,|\eta|} \qquad b = \frac{2}{3\,|\Delta|}$$

$$u_0 = u(0) \qquad u_1 = u(x_1)$$

$$v_1 = v(x_1) \qquad v_2 = v(x_2)$$

the coefficients of the equations system (18) are

$$c_{11} = 1 \qquad c_{12} = -\sqrt{u_0}\; J_{1/3}(au_0^{3/2})$$

$$c_{13} = -\sqrt{u_0}\; J_{-1/3}(au_0^{3/2}) \qquad c_{14} = 0$$

$$c_{15} = 0 \qquad c_{16} = 0 \qquad c_{21} = \gamma$$

$$c_{22} = -\frac{\eta}{|\eta|}\, u_0\, J_{-2/3}(au_0^{3/2}) \qquad c_{23} = \frac{\eta}{|\eta|}\, u_0\, J_{2/3}(au^{3/2})$$

$$c_{24} = 0 \qquad c_{25} = 0 \qquad c_{26} = 0 \qquad c_{31} = 0$$

$$c_{32} = \sqrt{u_1}\; J_{1/3}(au_1^{3/2}) \qquad c_{33} = \sqrt{u_1}\; J_{-1/3}(au_1^{3/2})$$

$$c_{34} = -\sqrt{v_1}\; J_{1/3}(bv_1^{3/2}) \qquad c_{35} = -\sqrt{v_1}\; J_{-1/3}(bv_1^{3/2})$$

$$c_{36} = 0 \qquad c_{41} = 0 \qquad c_{42} = \frac{\eta}{|\eta|}\, u_1\, J_{-2/3}(au_1^{3/2})$$

$$c_{43} = -\frac{\eta}{|\eta|}\, u_1\, J_{2/3}(au_1^{3/2})$$

$$c_{44} = -\frac{\Delta}{|\Delta|}\, v_1\, J_{-2/3}(bv_1^{3/2}) \qquad c_{45} = \frac{\Delta}{|\Delta|}\, v_1\, J_{2/3}(bv_1^{3/2})$$

$$c_{46} = 0 \qquad c_{51} = 0 \qquad c_{52} = 0 \qquad c_{53} = 0$$

$$c_{54} = \sqrt{v_2}\; J_{1/3}(bv_2^{3/2}) \qquad c_{55} = \sqrt{v_2}\; J_{-1/3}(bv_2^{3/2})$$

$$c_{56} = -1 \qquad c_{61} = 0 \qquad c_{62} = 0 \qquad c_{63} = 0$$

$$c_{64} = \frac{\Delta}{|\Delta|}\, v_2\, J_{-2/3}(bv_2^{3/2}) \qquad c_{65} = -\frac{\Delta}{|\Delta|}\, v_2\, J_{2/3}(bv_2^{3/2})$$

$$c_{66} = 0.$$

The amplitude coefficients related to A_1 are as follows:

$$\frac{A_2}{A_1} = -\frac{c_{11}c_{23} - c_{13}c_{21}}{c_{12}c_{23} - c_{13}c_{22}}$$

$$\frac{A_3}{A_1} = -\frac{c_{12}c_{21} - c_{11}c_{22}}{c_{12}c_{23} - c_{13}c_{22}}$$

$$\frac{A_4}{A_1} = -\frac{\left(c_{32}\frac{A_2}{A_1} + c_{33}\frac{A_3}{A_1}\right)c_{45} - \left(c_{42}\frac{A_2}{A_1} + c_{43}\frac{A_3}{A_1}\right)c_{35}}{c_{34}c_{45} - c_{35}c_{44}}$$

$$\frac{A_5}{A_1} = -\frac{\left(c_{42}\frac{A_2}{A_1} + c_{43}\frac{A_3}{A_1}\right)c_{34} - \left(c_{32}\frac{A_2}{A_1} + c_{33}\frac{A_3}{A_1}\right)c_{44}}{c_{34}c_{45} - c_{35}c_{44}}$$

$$\frac{A_6}{A_1} = -\frac{c_{54}\frac{A_4}{A_1} + c_{55}\frac{A_5}{A_1}}{c_{56}}.$$

The amplitude coefficient A_1 can be related to the total power P carried by the mode. The integral over the z component of the Poynting vector can be solved with the result

$$P = \frac{\beta A^2}{2\omega\mu_0}\left\{\frac{1}{2\gamma} + \frac{1}{2\theta}\left(\frac{A_6}{A_1}\right)^2 + \left(\frac{A_2}{A_1}\right)^2 I_1 + 2\,\frac{A_2A_3}{A_1^2}\, I_2 + \left(\frac{A_3}{A_1}\right)^2 I_3 + \left(\frac{A_4}{A_1}\right)^2 I_4 + 2\,\frac{A_4A_5}{A_1^2}\, I_5 + \left(\frac{A_5}{A_1}\right)^2 I_6\right\}$$

$$I_1 = \frac{1}{\eta}\,(u_1c_{32}^2 + c_{42}^2 - u_0c_{12}^2 - c_{22}^2)$$

$$I_2 = \frac{1}{\eta}\,(u_1c_{32}c_{33} + c_{42}c_{43} - u_0c_{12}c_{13} - c_{22}c_{23})$$

$$I_3 = \frac{1}{\eta}\,(u_1c_{33}^2 + c_{43}^2 - u_0c_{13}^2 - c_{23}^2)$$

$$I_4 = \frac{1}{\Delta}\,(v_2c_{54}^2 + c_{64}^2 - v_1c_{34}^2 - c_{44}^2)$$

$$I_5 = \frac{1}{\Delta}\,(v_2c_{54}c_{55} + c_{64}c_{65} - v_1c_{34}c_{35} - c_{44}c_{45})$$

$$I_6 = \frac{1}{\Delta}\,(v_2c_{55}^2 + c_{65}^2 - v_1c_{35}^2 - c_{45}^2).$$

References

[1] S. E. Miller, "Integrated optics: An introduction," *Bell Syst. Tech. J.*, vol. 48, no. 7, pp. 2059–2069, Sept. 1969.

[2] J. E. Goell and R. D. Standley, "Sputtered glass wave-guide for integrated optical circuits," *Bell Syst. Tech. J.*, vol. 48, no. 10, pp. 3445–3448, Dec. 1969.

[3] R. Ulrich, H. P. Weber, E. A. Chandros, W. J. Tomlinson, and E. A. Franke, "Embossed optical waveguides," *Appl. Phys. Lett.*, vol. 20, no. 6, pp. 213–215, Mar. 15, 1972.

[4] D. Marcuse, "Coupling coefficients for imperfect asymmetric slab waveguides," *Bell Syst. Tech. J.*, vol. 52, no. 1, pp. 63–82, Jan. 1973.

[5] I. P. Kaminow and J. R. Carruthers, "Optical waveguiding layers in $LiNbO_3$ and $LiTaO_3$," *Appl. Phys. Lett.*, vol. 22, no. 7, pp. 326–328, Apr. 1973.

[6] D. Marcuse, *Light Transmission Optics*. New York: Van Nostrand-Reinhold, 1972.

[7] P. M. Morse and H. Feshbach, *Methods of Theoretical Physics*, vol. II. New York: McGraw-Hill, 1953.